Int. J. Heat Mass Transfer. Vol. 18, pp. 513–526. Pergamon Press 1975. Printed in Great Britain

THE TRANSITION OF PLANE PLUMES

R. G. BILL, JR. and B. GEBHART
Sibley School of Mechanical and Aerospace Engineering, Upson Hall, Cornell University, Ithaca, NY 14850, U.S.A.

(*Received* 8 *April* 1974 *and in revised form* 25 *July* 1974)

Abstract—An experimental study of the transition of plane thermal plumes has clarified some of the mechanisms and indicated the limits of the transition regime in air. A flow subject to naturally occurring disturbances was found to selectively amplify disturbance components below a certain cutoff frequency. This is in agreement with a previous experimental study with controlled disturbances. There is apparently no narrow band-filtering, as found both for flows adjacent to vertical surfaces both from stability analysis and experiments. Nonlinear mechanisms arise to distribute disturbance energy both to higher frequencies and more uniformly across a broad spectrum. Turbulence intensity increases, then decreases. Such weak free-boundary flows are subjected to many disturbance sources and it was found necessary to be very careful in interpreting observed flow fluctuations as turbulence. A visual criterion, along with one based on the maximum instantaneous mid-plane temperature, proved reliable.

NOMENCLATURE

c_p, specific heat of fluid;
d, source wire diameter;
f, stream function;
g, gravitational acceleration;
G, stability, Grashof number, $4(Gr_x/4)^{1/4}$;
Gr_x, Grashof number based on temperature, $g\tilde{\beta}x^3\Delta t/\nu^2$;
$Gr_{Q',x}$, Grashof number based on heat flux, $g\tilde{\beta}x^3Q'\rho\nu^3c_p$;
$h(0)$, eigenvalue from laminar plume formulation of Fujii [6];
h, heat-transfer coefficient;
I, Prandtl number dependent variable of Gebhart *et al.* [21], $\int_{-\infty}^{\infty} f'\phi\,\mathrm{d}\eta$;
k, thermal conductivity of source wire;
L, length of source wire;
Q', heat flux/unit length;
t_0, plume midplane temperature;
t_∞, ambient fluid temperature;
U, x velocity component;
V, y velocity component;
x, vertical distance above line source;
y, horizontal distance from plume midplane.

Greek symbols

$\bar{\beta}$, disturbance frequency;
β, non-dimensionalized frequency, $\delta\bar{\beta}/U$;
$\tilde{\beta}$, volumetric temperature coefficient of fluid;
δ, boundary-layer thickness parameter, $4x/G$;
η, similarity variable of Gebhart *et al.* [21], $y/x(Gr_x/4)^{1/4}$;
μ, fluid viscosity;
ν, kinematic fluid viscosity;
ρ, fluid density;
ϕ, non-dimensionalized temperature excess, $\dfrac{t-t_\infty}{t_0-t_\infty}$.

1. INTRODUCTION

SINCE the theoretical paper of Zel'dovich [1], laminar and turbulent plumes arising from horizontal line sources of buoyancy have been the subject of many investigations. Zel'dovich, using similarity methods employed by Tollmien [2] and Schlichting [3], developed temperature and velocity similarity forms for plane and axisymmetric plumes in both the laminar and turbulent regimes. Subsequently, similarity solutions from the laminar boundary layer equations have been published by many authors for different Prandtl numbers. Gebhart, Pera and Schorr [4] reviewed these studies for plane plumes and simplified the formulation. Numerical results were given for Prandtl numbers in the range from 0·01 to 100·0. More recently, Fujii *et al.* [5] increased the accuracy of the numerical results over those of Fujii [6] and of Gebhart *et al.* [4].

Experimental studies of laminar plane plumes include those of Brodowicz and Kierkus [7] and Forstrom and Sparrow [8] in air and of Schorr and Gebhart [9] in a silicone oil. Temperature measurements were in good agreement with the laminar theory, except for an almost uniform 15 per cent deficiency in the midplace temperature. Fujii *et al.* [5] corroborated the results in air. However, in spindle oil and in water, they found, for $Gr_x < 2{\cdot}3 \times 10^4$, that the

centerline temperature was in good agreement with laminar theory. The measurements of Lyakhov [10] in air indicated that the centerline temperature is increased to 2·4 per cent above the theoretical value by bounding the space below the line source with an impermeable plate. Lyakhov noted that this is more consistent with the laminar boundary approximation which does not anticipate the flow now known to be induced below the level of the source.

Many observations of laminar plume flow have indicated that they sway in a plane perpendicular to the axis of the source. Another mode of instability was noted by Miaybe and Katsuhara [11]. They reported sinusoidal oscillations, of a plume in spindle oil, in the transverse direction, i.e. across the span of the plane plume.

Pera and Gebhart [12] have shown that initial instability of plane plumes to two-dimensional disturbances may be analyzed by linear stability theory. This theory predicts the amplification characteristics of small periodic disturbances in the boundary region flow as a function of frequency β and Grashof number Gr_x. See Gebhart [13] for a discussion concerning the flows which have been considered in detail. Pera and Gebhart [12] developed the coupled Orr–Sommerfeld type equations using a parallel flow approximation and considered disturbances of both a symmetric and asymmetric nature, through the use of separate sets of boundary conditions. General disturbances may be considered to be linear combinations of these two types, see Fig. 1.

The stability equations were integrated numerically. A portion of the neutral stability curve for air, $Pr = 0{\cdot}7$, is seen in Fig. 2. In the inviscid limit, it was found

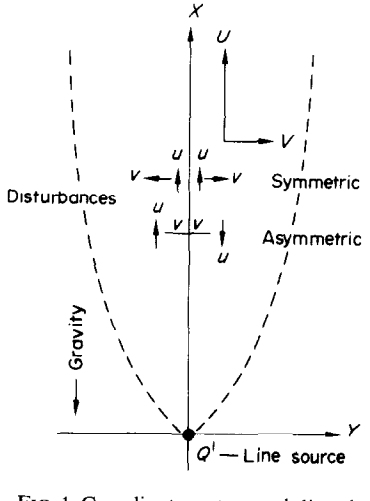

FIG. 1. Coordinate system and disturbance definitions.

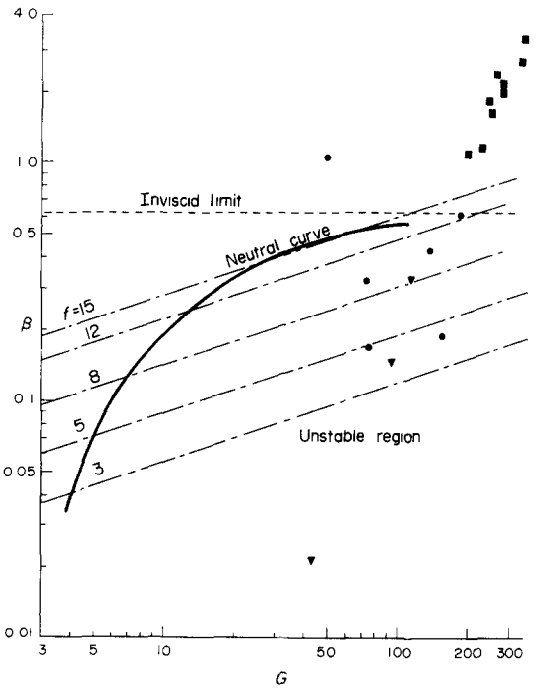

FIG. 2. Computed neutral stability curve, Pera and Gebhart [12]. Constant frequency contours for air for $Q' = 58{\cdot}6$ Btu/h-ft. Data of highest frequency velocity disturbances. ●, $Q' = 68{\cdot}5$ Btu/h-ft; ■, $Q' = 68{\cdot}5$ Btu/h-ft (turbulent flow); ▼, $Q' = 3{\cdot}23$ Btu/h-ft.

that this flow was more stable to symmetric disturbances than to asymmetric ones. Hence the full equations were integrated only for the latter. The inviscid limit of β, shown in Fig. 2 for $Pr = 0{\cdot}7$, was found to be Prandtl number dependent with a minimum at $Pr = 1{\cdot}0$. Incidentally, disturbance coupling through buoyancy has the largest destabilizing effect at small G.

We here define G, β and the characteristic velocity U and length δ, in terms of $\Delta t = t_0 - t_\infty$, as:

$$G = 4\sqrt[4]{\left(\frac{Gr_x}{4}\right)} = 4\sqrt[4]{\left(\frac{g\bar{\beta}x^3\Delta t}{4\nu^2}\right)}$$

$$U = \frac{\nu G^2}{4x}; \qquad \delta = \frac{4x}{G}$$

$$\beta = \frac{\delta\bar{\beta}}{U} \propto \bar{\beta}G^{1/3}.$$

Thus, constant physical frequency lines are as shown on Fig. 2, for a heat input Q' of 58·6 Btu/h-ft [56·3 W/m]. For an initially small disturbance, nonlinear effects should not arise and its frequency should be conserved as it is convected downstream. These lines then are downstream paths of linear disturbance propagation. This plot predicts that all frequencies

greater than 15 Hz should be damped for this Q'. For any given heat input, and perhaps for any fluid, there is a frequency level below which all disturbances are amplified.

Pera and Gebhart [12] checked these predictions by introducing artificial asymmetric disturbances into a plume of air above a 6 in (15·2 cm) long electrically heated wire. Using a hot-wire, disturbances of frequencies higher than 12 Hz were not found to survive downstream for $Q' = 58{\cdot}6$ Btu/h-ft. This favorable comparison with the predictions of linear stability theory led the authors to suggest that the discrepancy in the limiting frequency may be due to imperfections in the form of the disturbances introduced. Incidently, it was not possible to experimentally determine the location of the neutral curve because the low values of G were very close to the plume source, for that experiment in atmospheric air.

Recently Haaland and Sparrow [14] have repeated the calculations of Pera and Gebhart [12], retaining two of the several terms usually neglected in stability analysis but which may be included without disturbing similarity in terms of G. The principal result is a lower branch of the neutral curve very near the horizontal axis. The consequence of this lower branch is the prediction of frequency filtering for the plane plume flow, as found initially by Dring and Gebhart [15] for flow adjacent to a vertical surface.

With increasing G, the stability results of Pera and Gebhart [12] should asymptotically approach those of Haaland and Sparrow [14]. Thus the existence of a lower branch occurring below the stability region calculated by Pera and Gebhart seems likely. Mahajan and Gebhart [16] recently reinvestigated the question of the existence of a lower branch. Using the same parallel flow approximation used in the formulation of Pera and Gebhart, their investigation confirmed the existence of a lower branch below the region calculated by Pera and Gebhart. Furthermore a band filtering mechanism was indicated. A plot of disturbance amplitude contours showed, however, that, for the range of Grashof numbers found to lead to turbulence in this experiment, the filtering is relatively weak and includes a much broader band of frequencies than the sharp filtering calculated by Dring and Gebhart [15]. Thus one does not expect velocity and temperature disturbances that lead to transition to be dominated by frequency filtering, as found by Jaluria and Gebhart [19] in transition on a vertical plate.

Mahajan and Gebhart [16] also determined corresponding constant disturbance amplitude contours from the amplification rate contours presented graphically by Haaland and Sparrow [14]. These contours also indicate a broad-band filtering mechanism. The results of [12] and [14] differ chiefly in the region of low Grashof number where both parallel flow and boundary layer approximations are invalid. However, the same picture, of broad-band filtering, results from both formulations.

In spite of the successful comparison of experimental and analytical results by Pera and Gebhart [12], linear stability theory does not *a priori* offer any prediction of flow events after disturbances are no longer of small amplitude. Nonlinear effects may quickly dominate the subsequent distribution of disturbance energy. Another possibility is that transverse disturbances may further complicate this two-dimensional flow.

Data relating to transition in plumes is quite sparse. Forstrom and Sparrow [8] generated flows sufficiently vigorous to disrupt the laminar patterns. Thermocouple measurements indicated turbulent bursts and their first appearance was taken as the beginning of transition. Characterizing the local vigor of the flow by a local Grashof number, based on the heat input rate, these occurred at $Gr_{Q',x} = 5 \times 10^8$.

At the highest heating rate used, and at the most distant location downstream, turbulent bursts were observed with great frequency. Furthermore, under this condition, a time-averaged temperature profile showed a thickening of the flow region, with respect to laminar flow. Based on this observation, Forstrom and Sparrow concluded that full turbulence occurred at $Gr_{Q',x} = 5 \times 10^9$. Only this single data point was taken in what was taken to be the turbulent region. No comparisons could be made with the temperature decay in x for turbulent plumes predicted by Zel'dovich [1]. Even though flow at the highest Grashof number was found to be primarily turbulent, the maximum centerline temperature of the plume still was found to follow the functional dependence on heat flux predicted by laminar theory. We note that temperature levels for laminar flow depend on $Q'^{4/5}$ while in turbulent flow (either plane or axisymmetric) the dependence is indicated to be at least approximately $Q'^{2/3}$.

The turbulent data taken by Rouse *et al.* [17] and by Lee and Emmons [18] are difficult to interpret as thermal-buoyancy induced line source plumes since in the former study the plume flow was generated by a row of gas burners and in the latter by burning liquid fuel in a channel burner. In both experiments the plume source was of appreciable size and introduced initial momentum flux, diffusing chemical species of different molecular weight, initial disturbances and nonuniformity of energy production rate. Results of Lee and Emmons are tabulated only in terms of the fuel consumption rate per unit length of burner.

The purpose of the present study was to bring together the various aspects of plane plume instability and transition that have been studied separately and independent of the total transition process. Using a

fine thermocouple and a hot wire anemometer probe, along with an interferometer, disturbances and turbulence conditions were studied in a plane plume subject to naturally occurring disturbances.

Our disturbance frequency data are in accord with the predictions of linear stability theory. Increasing local Grashof numbers was obtained either by increasing the heat input or by moving the probes further downstream. Velocity disturbance signals were decomposed with a spectrum analyzer. Somewhat surprisingly, it was found that all frequency components of appreciable amplitude fell in the amplified region of the stability plane, even to the end of transition. This indicates that linear stability considerations are important even in regions of large disturbance amplitude.

The plume was always visualized with a 20 cm aperture Mach–Zehnder interferometer. This was found to be extremely useful in interpreting the point data of the thermocouple and hot wire probes in terms of the general flow configuration. The region considered to have turbulent bursts by Forstrom and Sparrow was found to consist of a flow in which two-dimensional sinusoidal-like disturbances had reached large amplitudes and higher frequency disturbances had begun to appear. These large disturbances were seen to sweep away to leave a well-ordered and completely laminar boundary region. With increasing local Grashof number they became more frequent and eventually the laminar boundary layer broke down completely.

This corresponds to the condition for which Forstrom and Sparrow reported a thickening of the profile and concluded the presence of complete turbulence. Yet, in the flow regime upstream of this last condition, the maximum instantaneous midplane temperature was still decreasing both downstream and with plume heat input as predicted by the laminar theory. Further downstream, the changing centerline temperature finally came to depend on turbulent field parameters. In these observations, above a 10 in (25·4 cm) electrically heated wire at different downstream locations, and for six different heat input levels, these events occurred at roughly the same values of the local Grashof number. Thus, the beginning and end of transition both correlated in terms of this parameter.

Some of the patterns already established for transition adjacent to a vertical surface, Jaluria and Gebhart [19], are paralleled by our data. Two-dimensional disturbances were found to amplify selectively, as predicted to be unstable. At increasing amplitude, three-dimensional effects became apparent. However, no delayed thermal transition effect was observed. This might be expected in air, $Pr = 0{\cdot}7$, since velocity and temperature disturbances appear to grow together and remain coupled. After a period of intermittancy the flow adjusts to turbulent parameters.

2. THE EXPERIMENT

Our experiments were performed in atmospheric air, for obvious advantages as well as for simplicity with the Mach–Zehnder. The major disadvantage of the use of air is the high source-wire temperatures (approximately 1000°F) necessary to achieve the vigor of flow required for transition. Radiation from the source becomes a significant and somewhat uncertain correction which must be applied in order to know Q'. Moreover, the high air temperatures made very accurate absolute calibration of the hot wire probe infeasible.

The sources used in this experiment were formed on the wire holder pictured by Schorr and Gebhart [9]. Wire lengths of 10, 6, 2 and 1 in (25·4, 15·2, 5·1 and 2·5 cm) were successively stretched across the holder. The wire material and diameter used for each length are shown in Table 1.

Table 1

Material	Source length	Diameter d (in)	L/d
Alumel	10	0·0135	741
Alumel	6	0·0135	445
Nichrome	2	0·005	400
Nichrome	1	0·0025	400

The wire materials were chosen so that the wire remained taut in the holder under all heating conditions. Increased length was taken up by the spring-like deflection of the support. The high resistivity nichrome wire made it possible to obtain the necessary high power inputs at low amperage. High currents would have caused heating at the current leads and connections and thus would have generated additional weak plumes.

The experiment was enclosed in a test enclosure of dimensions $24 \times 29 \times 45$ in ($61{\cdot}0 \times 73{\cdot}7 \times 114{\cdot}3$ cm) high which had louvered vents (11×13 in) $27{\cdot}9 \times 33{\cdot}0$ cm) centered in the roof and floor. The test beam of the interferometer traversed the test section through two 8 in (20·3 cm) diameter interferometer grade windows which were mounted to the test section in spring-loaded frames designed to allow changes in the angular orientation of the windows. Translation and rotation of the wire source within the enclosure was accomplished through the tripod mounting external to the enclosure. The room in which the experiments were performed was isolated from large temperature changes by insulated walls. The daily room temperature variations were only 2–3°F (1–2°C).

The interferometer is similar to that described by Gebhart and Knowles [20] and the light source was a 100 W low-density mercury vapor thermal source. The light was passed through a green interference filter (5461Å), in order to provide sharp fringes. Photographic data were taken on 35 mm Kodak Tri-X Pan film (ASA 400) using a LeicaFlex SL single lens reflex camera with Focusing Bellows(R) attachment for fine focusing. A grid with vertical and horizontal spacings of 1/2 in (1·3 cm) was placed in the test section for distance determination. The plume source was positioned parallel to the collimated light beam by optical means.

Electrical power, provided by a stabilized Nobatron MR36-30, was determined from the voltage drop across the wire and by calculating the current from the voltage drop across a Leeds and Northrup 0·1 Ω calibrated shunt resistor. A Dana Digital Voltmeter 4800 was used.

The hot-wire sensor was pure platinum, of 0·001 in dia (0·0025 cm), with standard Disa probe supports and connectors. A differential traversing mechanism allowed the hot wire to be moved in the horizontal plane perpendicular to the line source. The electronics, a Disa 55D01 unit, was operated at an overheat ratio of 1·3. Our interest was in qualitative characteristics. The sensor axis was parallel to the wire source and its signal, therefore, represents the sum of the U and V velocity components, as shown in Fig. 1. Hot wire output was recorded on a Beckman type R Dynograph Recorder.

The thermocouple probe was an Omega Chromel–Constantan, made from 0·001 in (0·0025 cm) diameter wire. An ice reference junction was used. All circuit connections were made using Omega 24 gauge chromel and constantan wire. The thermocouple leads were extended along the hot wire probe support and its junction was approximately 1/4 in (0·6 cm) from the end of a 1/16 in (0·2 cm) rod support. The junction was in the same horizontal plane as the hot wire sensor and separated from it by a distance of 2 in (5·1 cm) in the spanwise direction. A comparison of actual thermocouple output with the Omega Chromel and Constantan thermocouple tables at temperatures of 69°F in air and 125°F water bath, showed agreement to 0·5 per cent. Thermocouple output was also recorded on a Beckman type R Dynograph Recorder.

For low local Grashof number flow, the signals of the hot wire and thermocouple were characterized by disturbances with peaks occurring at frequencies less than 1 Hz. However, at higher values, the principal frequencies were much higher. Under these conditions a General Radio Company Sound and Vibration Analyzer (1564A) determined the root mean square of the frequency spectrum of the hot wire output. The analyzer range, from 2·5 Hz to 25 000 Hz, is scanned in 5 min. The output was recorded on a General Radio Company Graphic Level Recorder (1521-B).

The calibrations of the analyzer and recorder were checked by introducing sinusoidal signals from a Hewlitt Packard 3300A Function Generator. The amplitude of the signal was measured on the Beckman recorder. The noise level of the hot wire anemometer unit was determined by analyzing the hot wire signal at no fluid motion.

Before the beginning of each experiment, the ambient temperature of the air in the test section was measured. The temperature of the ambient air increased during plume measurements but soon returned to the original temperature. Vertical traverses of the test section indicated that there was no appreciable thermal stratification in the ambient medium.

For each heat input, measurements were taken from 1 in (2·5 cm) to 30 in (76·2 cm) above the heat source. However, visual observations were limited to a distance up to 15 in (38·1 cm) above the source, because of test section constraints. When the 10 in source was used, the hot wire and thermocouple probes were each positioned 1 in on opposite sides of the middle of the heat source span. For the shorter sources, it was desired to have the exact midplane temperatures of the plume at midspan, due to the possibility of significant end effects. Therefore, only the thermocouple was used and it was positioned, with the aid of a plumb bob, at midspan of the heat source. The convective part of the heat input for the experiments was varied from 13·5 to 103·6 Btu/h-ft (13·0–99·6 W/m).

At a given heat input, the transition of the plume from laminar to turbulent flow was viewed through the single-lens reflex camera. In this way, the changes in the flow regime were viewed continuously and pictures were taken as thought appropriate.

3. RESULTS AND OBSERVATIONS

Heat-transfer evaluations

The electrical energy supplied to the wire source was dissipated to the surroundings by axial conduction to the wire holder, radiation to the enclosure and convection to the fluid around the wire. According to Schorr and Gebhart [9] the ratio of the heat loss by end conduction to the total heat generated is estimated as

$$\frac{Q'_{\text{conduction}}}{Q'_{\text{generated}}} = \frac{kd}{hL^2}$$

where h is the heat-transfer coefficient, k is the thermal conductivity of the wire, d is the diameter of the wire and L is its length. Calculating h from Gebhart and Pera [21], the ratio for the 10, 6, 2 and 1 in wires is 0·3, 0·8, 2·5 and 0·9 per cent, respectively. This correction was neglected.

The large spread of emissivity data for both alumel and nichrome in Gubareff *et al.* [22] made it impossible to calculate the radiation loss with confidence. The convective heat flow of the plume was inferred by measuring the mid-plane temperature in regions of steady laminar flow with a fine thermocouple and then calculating Q' from the laminar boundary-layer plume formulation of Gebhart *et al.* [4], with a 15 per cent correction to the measured temperature. For all levels of electrical heating used in this experiment, the heat flux inferred from corrected laminar theory was within 5 per cent of the electrical input.

Temperature measurement

The time variations of the mid-plane velocity and temperature for different values of the local Grashof number, actually $G = 4\sqrt[4]{(Gr_x/4)}$, for the 10 in source and a heat input level of 35·8 Btu/h-ft (34·4 W/m), are shown in Fig. 3. Increasing values of G were obtained at increasingly downstream locations of measurement. Time variations of the hot wire and thermocouple signals, in Figs. 3(a) and (b), clearly indicate that velocity and temperature disturbances are strongly coupled. The time scale is 0·1 cm/s for each record; however, the recorder gain levels in (a), (b) and (c) are different.

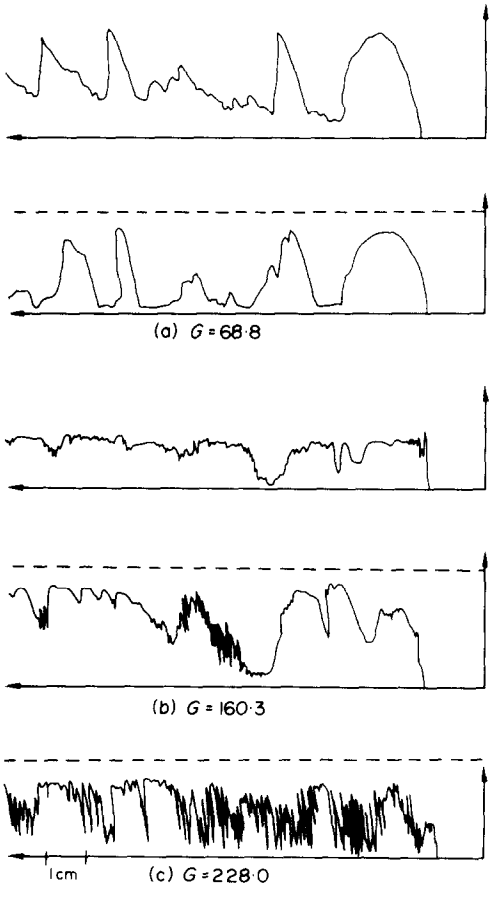

FIG. 3. Time variation of hot wire and thermocouple outputs, respectively, at $G = 68{\cdot}8$ and 160·3 and thermocouple output at $G = 228{\cdot}0$, ——— laminar theory.

In Fig. 3(a) ($G = 68{\cdot}8$), the temperature disturbances have frequencies of the order of 0·2 Hz or less. The temperature level varies from its maximum almost down to the ambient, which is the level of the horizontal axis. These large fluctuations were seen, in the interferometer, to result from the swaying of the plume perpendicular to its average midplane, as well as from oscillations along its span. Despite these disturbances, the plume appeared to remain primarily laminar as seen in Fig. 4(a), where the listed local value of G applies at the level of the arrow. In Fig. 4(b) the flow is apparently still laminar, despite large spanwise distortion.

With increasing Grashof number, small amplitude higher frequency disturbances begin to appear in the thermocouple and hot wire outputs, as seen in Fig. 3(b). These are superimposed on the higher amplitude low frequency disturbances seen at lower Grashof number. Simultaneously, large unsteady and wave-like disturbances were visible in the interferometer, as seen in Fig. 4(c), immediately downstream of the arrow marking the local value $G = 186$. These occurrences are very complicated. They are taken as the first signs of local turbulence and are defined as the beginning of transition.

In the transition region the laminar flow was intermittently disturbed by the passage of disturbances, followed by relaminarization. Further downstream, disturbance frequency and amplitude increased. The end of transition was taken as the location in x at which a thickening of the mean flow boundary layer and no relaminarization occurred [see Fig. 4(c)].

Beyond the end of transition, the thermocouple and hot-wire outputs were dominated by high frequency components, as seen in Fig. 3(c). The turbulent condition seen in Fig. 4(d) is characterized by a thickened boundary layer and a chaotic temperature field. The arrow is at the same local Grashof number as for Fig. 3(c).

We did not study the statistical nature of the temperature and velocity disturbances at this point in our investigation but in all regions took the maximum measured instantaneous local temperature as characteristic of the flow there. These temperatures are plotted in the generalized form which results from the laminar plume formulation of Gebhart *et al.* [4] as follows:

$$T = \frac{t_0 - t_\infty}{Q'} \cdot 4(\sqrt{2})(\mu c_p I) = Gr_x^{-1/4} \qquad (1)$$

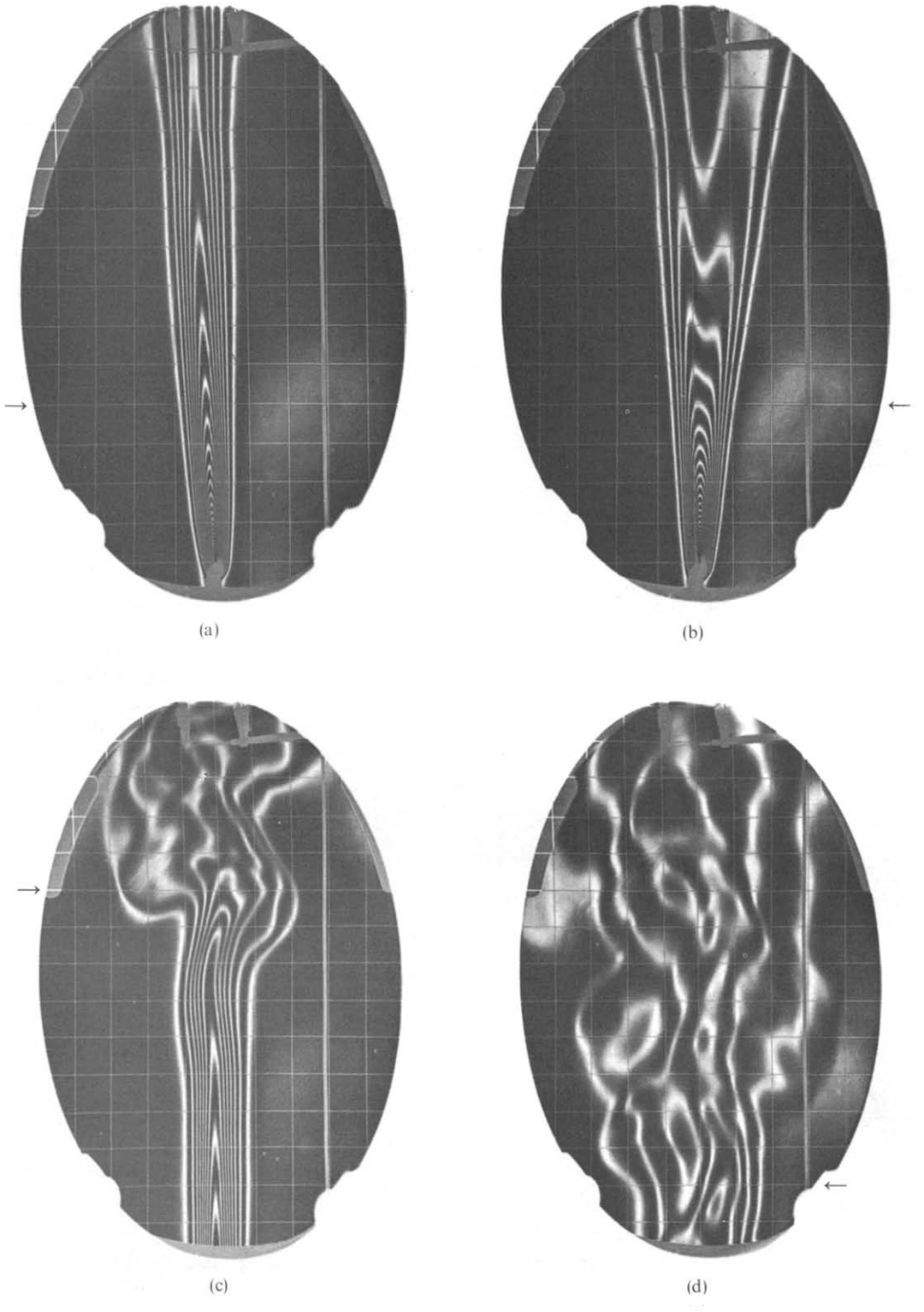

FIG. 4. Interferograms, $L = 10$ in. $G = 68{\cdot}8$, $68{\cdot}8$, $186{\cdot}0$ and $228{\cdot}0$ at arrow locations, respectively, which are $x = 2$, 8 and 12, respectively. $Q' = 52{\cdot}0$, $52{\cdot}0$, $102{\cdot}0$, $102{\cdot}0$ Btu/h-ft.

where I, found from the similarity solution, is Prandtl number dependent and is 0·623 for $Pr = 0{\cdot}7$.

For a turbulent plane plume, the centerline temperature dependence on the distance x downstream and heat flux was first estimated by Zel'dovich [1] and since re-established by others. When written in the above variables, this variation is

$$T = \frac{t_0 - t_\infty}{Q'} \cdot 4(\sqrt{2})(\mu c_p I) \propto I \cdot Gr_x^{-1/2}. \quad (2)$$

As suggested by Schorr and Gebhart [9], it is also interesting to compare plane plume temperatures with the theory for laminar and turbulent axisymmetric plumes. These results, of Fujii [6] which cover a wide range of Prandtl numbers for the laminar plume, and of Zel'dovich [1] for the turbulent plume are, respectively:

$$T = \frac{t_0 - t_\infty}{Q'} \cdot 4(\sqrt{2})(\mu c_p I)$$

$$= Gr_x^{-1/2} Q'^{1/2} \frac{(4 \times h(0)^3 L^3 I^2 g\tilde{\beta})^{1/2}}{(\pi^3 \rho c_p \nu^3)^{1/2}} \quad (3)$$

$$T = \frac{t_0 - t_\infty}{Q'} \cdot 4(\sqrt{2})(\mu c_p I)$$

$$\propto Gr_x^{-5/4} Q'^{1/2} (L^3 I g\tilde{\beta}/\rho c_p \nu^3)^{1/2}. \quad (4)$$

The mid-plane temperature data are shown in Fig. 5 from previous studies in air as well as from our results for $L = 10$ in, for all non-turbulent flow. Figures 6–9 show our additional results for 10, 6, 2 and 1 in length sources, respectively. These data are compared with laminar and turbulent theories. The deviation from laminar theory, the 15 per cent deficiency in mid-plane temperature noted above, is also shown. Property values were evaluated at the average of the maximum and ambient temperature.

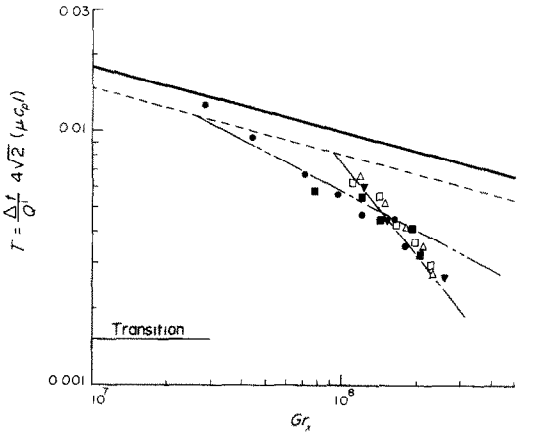

FIG. 6. T vs Gr_x for $L = 10$ in for turbulent plumes. ———, Laminar theory, plane plume; – – – –, Turbulent theory, plane plume; ——, Turbulent theory, axisymmetric plume; — — —, Experimental correction. ●, $Q' = 52{\cdot}0$ Btu/h-ft; ■, $Q' = 65{\cdot}8$ Btu/h-ft; △, $Q' = 78{\cdot}0$ Btu/h-ft; □, $Q' = 88{\cdot}0$ Btu/h-ft; ▼, $Q' = 102{\cdot}0$ Btu/h-ft.

Along with our data in Fig. 5 are the results of two past studies in air. The data points of Fujii *et al.* [5] in air, water, and spindle oil and of Schorr and Gebhart [9] in silicone oil are not plotted since they were not tabulated. However, they follow the same trends.

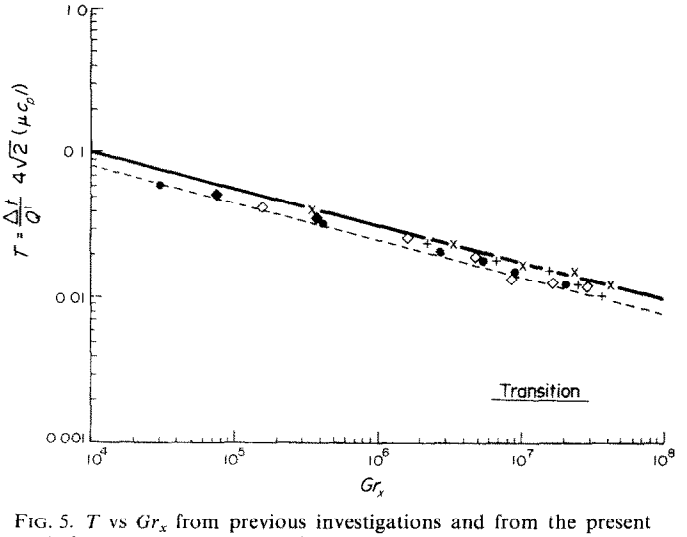

FIG. 5. T vs Gr_x from previous investigations and from the present study for $L = 10$ in, for non-turbulent plane plumes. ———, Laminar theory, plane plume; — — —, Experimental correction ◇, $Q' = 13.5$ Btu/h-ft; +, $Q' = 20{\cdot}6$ Btu/h-ft; ×, $Q' = 35{\cdot}8$ Btu/h-ft; ●, Forstrom and Sparrow [8], air; ◆, Brodowicz and Kierkus [7], air.

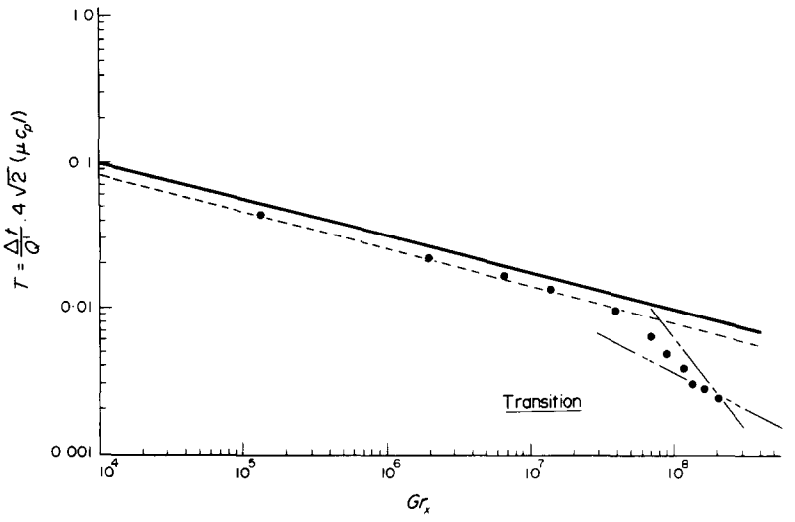

FIG. 7. T vs Gr_x for $L = 6$ in and $Q' = 103{\cdot}6$ Btu/h-ft, for laminar to turbulent flow conditions. ———, Laminar theory, plane plume; — — —, Turbulent theory, plane plume; – – –, Turbulent theory, axisymmetric plume; — — —, Experimental correction.

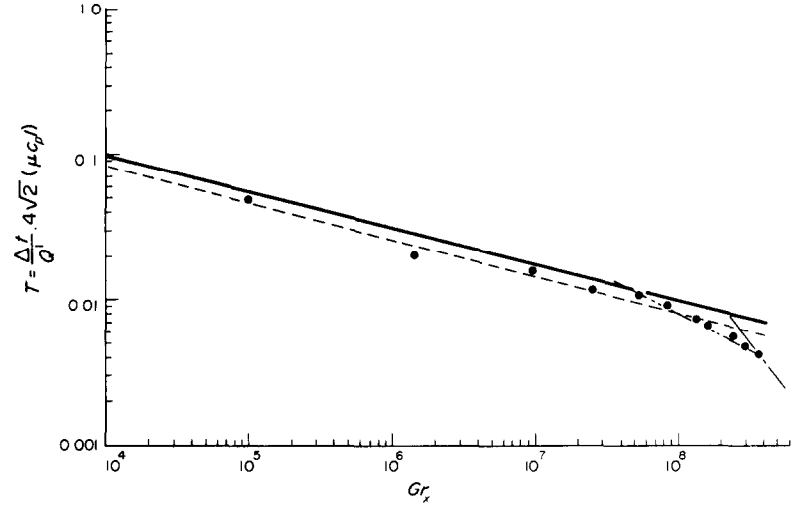

FIG. 8. T vs Gr_x for $L = 2$ in and $Q' = 91{\cdot}2$ Btu/h-ft, for laminar to turbulent flow conditions. ———, Laminar theory, plane plume; — — —, Turbulent theory, plane plume; – – –, Turbulent theory, axisymmetric plume; — — —, Experimental correction.

Our temperature maxima in Fig. 5 are in good agreement with the functional x dependence found by previous investigators [7, 8]. The data is generally above the line corresponding to the 15 per cent deficiency in mid-plane temperatures, even though the heat flux, which was inferred from mid-plane temperatures measured in the undisturbed laminar region of the plume, was calculated to correspond to a mid-plane temperature 15 per cent below the predictions of laminar boundary-layer theory. Thus the scatter implies that the maximum mid-plane temperatures encountered in disturbed regions of flow are not uniformly 15 per cent below laminar theory. The region of transition is indicated on Fig. 5. The persistence of the laminar temperature level through transition confirms the intermittently laminar nature of the flow.

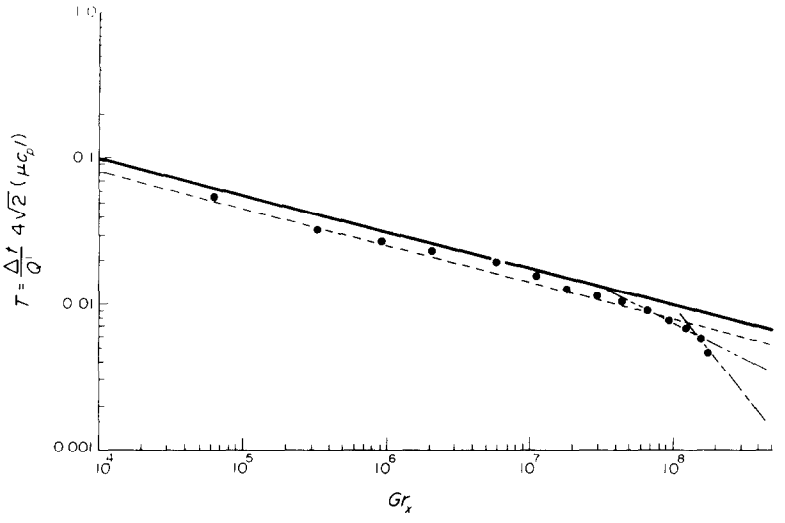

FIG. 9. T vs Gr_x for $L = 1$ in and $Q' = 47{\cdot}0$ Btu/h-ft, for laminar to turbulent flow conditions. ———, Laminar theory, plane plume; – – – –, Turbulent theory, plane plume; – – – –, Turbulent theory, axisymmetric plume; – · – ·, Experimental correction.

The mid-plane temperature results in Fig. 6 are for completely turbulent flow, for $L = 10$ in and for five different heat input levels. For Gr_x less than about 3×10^7, instantaneous temperature levels close to laminar theory are still achieved. However, beyond this, a substantial and systematic deviation occurs. The variation of T is also shown for both the plane and axisymmetric turbulent plumes. Since these theories only indicate the dependence on Gr_x within an unknown constant of proportionality, the curves were placed to best agree with our data. For the plane turbulent plume, T is only a function of Grashof number. However, in the axisymmetric flow, there is also a further dependence on $Q'^{1/2}$.

The data does not appear to correlate well with either theory alone. Immediately after the end of transition the data conforms most closely to turbulent plane plume behavior. At higher Grashof numbers, the slope of the data decreases further and conforms most closely to the trend for an axisymmetric plume. However, the data does not show any systematic Q' dependence. The theories for turbulent plumes have been derived for mean flow values and neither their accuracy nor their applicability to temperature maxima are established.

Figure 7 is a similar plot of our mid-plane data above sources with $L = 6$ in, for the single heat input of 103·6 Btu/h-ft (99·6 W/m). Again the observed region of transition is noted. The laminar temperature level again persists through transition. Systematic deviations begin at about $Gr_x = 7 \times 10^7$. After transition, the centerline temperature does not at first decay according to either turbulent theory, although after $Gr_x = 1{\cdot}2 \times 10^8$, its slope conforms to that predicted for a turbulent plane plume.

This behavior is different than that for $L = 10$ in where the data in turbulent flow first follows closely the slope of turbulent plane plume theory and after $Gr_x = 1{\cdot}2 \times 10^8$ it follows more closely the slope predicted for turbulent axisymmetric plumes. A knowledge of the statistical relationship between maxima and mean flow quantities would perhaps remove this apparent inconsistency.

Because of the short optical length for the 2 and 1 in sources, it was not possible to make any visual observations. However, T vs Gr_x is plotted in Fig. 8 for the 2 in wire with the single heat input $Q' = 91{\cdot}2$ Btu/h-ft (87·7 W/m). Deviations from the corrected laminar theories do not occur until $Gr_x = 2{\cdot}0 \times 10^8$. Hence, until that point, it may be inferred that the flow was intermittently laminar, suggesting that this plume was more stable than those from the 10 and 6 in sources. The data at high values of Gr_x conforms closely to the prediction for the plane turbulent plume.

Our measurement for $L = 1$ in and $Q' = 47{\cdot}0$ Btu/h-ft (45·2 W/m) appear in Fig. 9. This flow again appears more stable than for $L = 6$ and 10 in, but less stable than that from a 2 in source. Deviations from corrected

laminar theory occur at $Gr_x = 1{\cdot}5 \times 10^8$. The data is not sufficient to make significant comparisons with turbulent theories.

Disturbance velocity spectra

The stability plane of Fig. 2 predicts that, at low Grashof numbers, disturbances of low frequency begin to amplify most quickly. Also, beyond an upper frequency limit, which is a function of the heat flux, they are damped. We would expect that in any experimental circumstance there are naturally occurring disturbances characterized by components covering a wide frequency range. Thus, the theory predicts that the flow will filter energy to disturbances below the frequency cut-off, while damping out those above.

Although available instrumentation did not allow the measurement of the entire spectrum, it was possible to determine disturbance spectra down to 2·5 Hz. Comparison of spectra at different Grashof number values indicated the range of frequencies which were amplified.

The locations in β, G coordinates of the highest disturbance frequencies observed for $L = 10$ in and at $Q' = 68{\cdot}5$ and 3·23 Btu/h-ft (65·9 and 3·2 W/m) are plotted in Fig. 2. The trend of the data with G indicates that disturbance energy is found at increasingly higher frequencies further downstream. We also see that all disturbances detected up to $G = 194$ have, with one exception, traversed the amplified region of the stability plane. This is almost to the end of transition which was about at $G = 208$. Beyond the end of transition, energy is found in higher frequencies, clearly indicating the kind of nonlinear disturbance growth and propagation mechanisms found by Jaluria and Gebhart [19] in flows adjacent to a vertical surface. The spread of observed frequencies for $G < 208$ does not indicate a narrow band filtering process.

The hot wire spectra were found to vary with time. We also note that the spectra for different local Grashof numbers do not result from following the disturbances as they are convected downstream. That is, larger G were obtained at larger x at different times. However, the general agreement of the data with stability theory indicates that the postulates of amplification and subsequent energy transfer into higher frequencies is plausible.

The spectra of hot wire signals are reproduced for the frequency range 2·5–100 Hz in Fig. 10. The spectra are; first for no flow, than for $G = 48$, 73·1, 153 and 194, all for $Q' = 65{\cdot}8$ Btu/h-ft (63·3 W/m) and $L = 10$ in. Recall that transition is complete at about $G = 208$. The spectra are RMS amplitude in volts vs frequency, along logarithmic coordinates. The spectrum with no fluid motion is of the noise output of the instrumentation system in a quiescent surrounding and provides a zero level against which we may detect the amplitude and frequency of signals caused by velocity disturbances.

The local flow condition for the spectrum of Fig. 10(b), $G = 48$, was primarily laminar. Peaks above the levels of Fig. 10(a) occur in this spectrum to as high as 65 Hz. Disturbances centered on 60 Hz also appear in each of the following spectra and are believed to be due to electronic noise. The highest frequency component at $G = 48$ that may be attributed to plume flow disturbances is at around 30 Hz. This frequency corresponds to a β of 1·11. The point, shown in Fig. 2 is clearly outside the amplified region.

The spectra of Figs. 10(b), (c) and (d) indicate that disturbance frequency components above perhaps 8·5 Hz are essentially unamplified up to $G = 153$. The presence of such disturbance components may result from external effects which enter the flow and are not sufficiently damped to be removed.

The flow conditions at $G = 73$ was still primarily laminar. As noted above, it is seen that only frequencies less than 8·5 Hz, $\beta = 0{\cdot}3515$, have been amplified above the disturbance levels at $G = 48$. In Fig. 2, this data point falls within the amplified region.

At $G = 153$, the flow has begun transition. Disturbance frequency components below 4·7 Hz ($\beta = 0{\cdot}1930$) now appear to have been highly amplified. The data point for 4·7 Hz, seen in Fig. 2, is still within the amplified region of the stability plane despite the large amplitude of these disturbances. The shifts in frequency of the most highly amplified disturbance components between Figs. 10(c) and 10(d) probably result from the unsteady nature of the disturbance mechanism.

The spectrum for a flow approaching the end of transition at $G = 194$, is seen in Fig. 10(e). Appreciable disturbance amplitude is found to have frequencies as high as 26 Hz, $\beta = 1{\cdot}13$, well above the neutral curve. Nonlinear mechanisms now control the disturbance spectrum and feed energy from both the mean flow and disturbances into higher frequency components.

As yet higher values of G the disturbance energy was found to spread to still higher frequencies, further broadening the spectrum. However, the disturbance amplitude at all frequencies diminished and the spectrum became uniformly filled out. This is the consequence of the enhanced entrainment, by turbulence, of fluid from the ambient surroundings, thus decreasing the energy per unit fluid mass. Another, but parallel, explanation of this result is possible. Initially, in first turbulence, the scale of the turbulence quickly becomes large. These large eddies are then quickly broken up to smaller ones. We note here, parenthetically, that the points designated by solid squares in Fig. 2 cor-

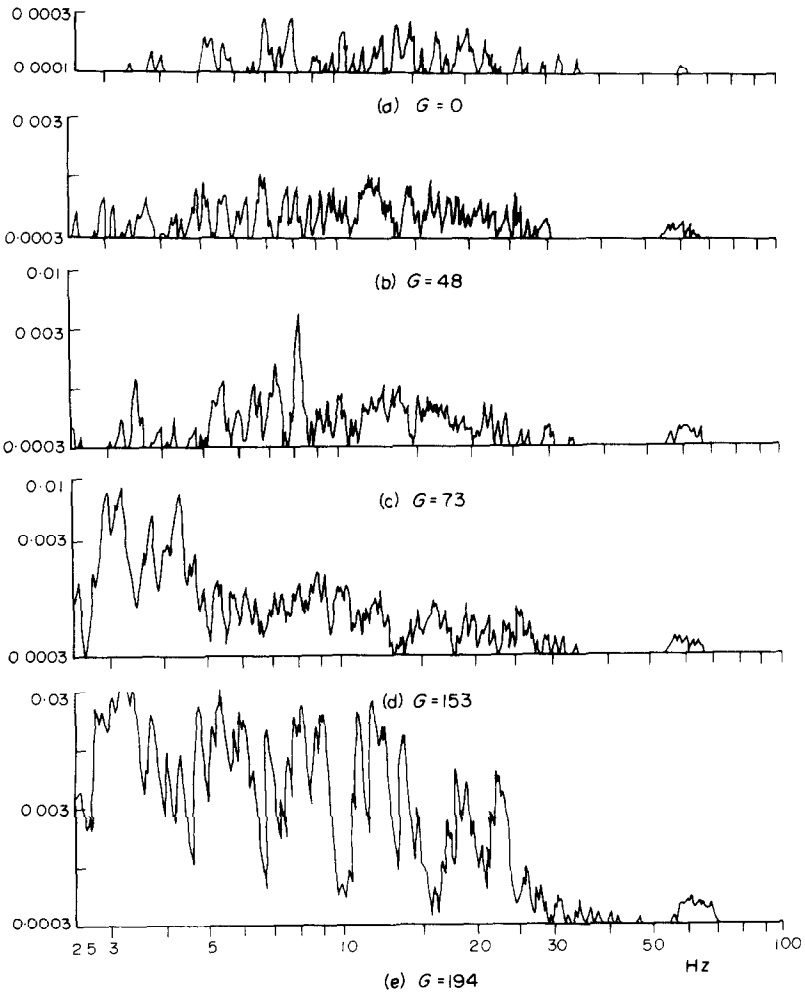

FIG. 10. Hot wire output spectra, volts^2 vs frequency, for $L = 10$ in, $Q' = 65{\cdot}8$ Btu/h-ft.

respond to completely turbulent flow. The values of β correspond to the highest frequency component found in the hot wire spectra.

In order to investigate the effect of heat input on stability, an experiment was performed with a Q' of 3·23 Btu/h-ft (3·2 W/m). Since, from the similarity solution, in the terms of Gebhart *et al.* [4], $\bar{\beta} \propto \beta G^{-1/3} Q'^{2/3}$, lower values of Q' should result in disturbances of lower frequency being amplified. The measured values shown in Fig. 2 were obtained from analog recordings of the hot wire signal. They also agree well with stability theory predictions.

Visual observations

As mentioned above, the transition limits noted in Figs. 5 and 7 were identified entirely from visual observations, not from changes in the character of the thermocouple and hot wire outputs. The importance of visual determination is apparent from a comparison of the thermocouple output in Fig. 3(a) ($G = 68{\cdot}8$) with the interferogram of Fig. 4(a), where the arrow indicates the plume position having the same G as that for Fig. 3(a). The sensors show disturbances of large amplitude. However, continuing observation of the interferogram indicated that these disturbances resulted from the swaying of the plume perpendicular to its average mid-plane and from oscillations along its span. They are not turbulent disruption of the flow. Although the thermocouple and hot wire signals indicate that the frequency and amplitude of the disturbances increase continuously with G, the large wave-like temperature disturbances were seen in the interferometer to have become very large at about $G = 142$ ($Gr_x = 6{\cdot}4 \times 10^6$) for both the 6 and 10 in sources.

These waves were not simply sinusoidal in the thermocouple and hot wire outputs and their spectra indicated that disturbance energy was distributed among many frequency components.

Local Grashof numbers at the end of transition were also visually determined by noting the location in x at which a thickening of the mean flow boundary layer occurred without relaminarization at later times. The results, tabulated in Table 2 for $L = 10$ in and for five different input rates Q', indicate that the end of transition correlates well with the single parameter Gr_x. The average value is $2{\cdot}95 \times 10^7$ ($G = 208$). The single data point for $L = 6$ in is also in close agreement with this value.

Table 2

L/d	L(in)	Q'(Btu/h-ft)	x(in)	Gr_x	G
741	10	13·5	17·0	$2{\cdot}95 \times 10^7$	208
741	10	20·6	14·0	$2{\cdot}50 \times 10^7$	200
741	10	35·8	12·5	$3{\cdot}52 \times 10^7$	218
741	10	51·5	11·0	$2{\cdot}83 \times 10^7$	207
741	10	70·5	9·5	$2{\cdot}96 \times 10^7$	208
444	6	103·6	10·5	$2{\cdot}17 \times 10^7$	190

Our estimates of the beginning and end of transition may be compared with those of Forstrom and Sparrow [8]. They reported bursts and the beginning of transition at $Gr_{Q',x} = 5{\cdot}0 \times 10^8$. Our value, in terms of $Gr_{Q',x}$, is $11{\cdot}2 \times 10^8$. This discrepancy may in part be due to the insensitivity of the integrated interferometer output to small local disturbances.

In terms of the heat flux Grashof number, our value for the end of transition is $Gr_{Q',x} = 7{\cdot}9 \times 10^9$. Forstrom and Sparrow reported a single data point in flow judged to be turbulent at $Gr_{Q',x} = 5{\cdot}0 \times 10^9$. Their criterion was a thickened temperature profile. This does not define a precise point for the completion of transition and, from our data, it appears that such a local flow was still within the transition region.

CONCLUSIONS

Boundary layer theory applied to the plane plume provides a completely deterministic model for steady state laminar flow conditions. In contrast, transition and turbulent flow patterns encountered in this study are stochastic in nature. The randomness in the flow pattern must enter from the fluctuations in the boundary conditions.

The fluctuations we observed, in terms of the spectra of the hot wire signals, may follow from slight variations in heat input to the source and/or from disturbances within the enclosure. Fluctuations, from whatever source, were found to be selectively amplified approximately as predicted by linear stability theory. Their presence resulted in Tollmien–Schlichting type waves followed by the eventual complete disruption of the well-ordered laminar flow. For both the 10 and 6 in sources the beginning of transition was found at $Gr_x = 6{\cdot}4 \times 10^7$. It was observed to end at approximately the single value $Gr_x = 2{\cdot}95 \times 10^8$.

The correlation of centerline temperature with laminar theory provided a strong and unequivocal standard for the determination of the end of transition. After the complete disruption of the boundary layer, the flow begins to adjust to turbulent parameters, and the laminar centerline temperature is no longer achieved. Nonlinear effects have become important and spread disturbance energy to frequencies above those of the initially amplified disturbances. Turbulence intensity and scale then begin to decrease.

Our temperature results for the four different source lengths indicates that flows above 2 and 1 in length sources are more stable than those from 10 and 6 in sources. As source length is decreased, the tendency of the plume toward an axisymmetric form may increase. This may favor symmetric disturbances over asymmetric ones which, according to linear stability, are more stable.

The lack of correlation of temperature maxima data in turbulent flows with the relevant approximate theories perhaps indicates that temperature characteristics are not a determining factor for the mean flow, as they are in the laminar and transition regimes.

Acknowledgements—The writers wish to acknowledge support for this research under National Science Foundation Grant GK18529.

REFERENCES

1. Y. B. Zel'dovich, Limiting laws of freely rising convection currents, *Zh. Eskp. Teoret. Fiz.* **7**, 1463 (1937).
2. W. Tollmien, Berechnung turbulenter Ausbreitungivorgange, *Z. Angew. Math. Mech.* **6**, 468 (1926).
3. H. Schlichting, Laminare Strahlausbreitung, *Z. Angew. Math. Mech.* **13**, 260 (1933).
4. B. Gebhart, L. Pera and A. W. Schorr, Steady laminar natural convection plume above a horizontal line heat source, *Int. J. Heat Mass Transfer* **13**, 161 (1970).
5. T. Fujii, I. Morioka and H. Uehara, Buoyant plume above a horizontal line heat source, *Int. J. Heat Mass Transfer* **16**, 755 (1973).
6. T. Fujii, Theory of steady laminar natural convection above a horizontal line heat source and a point heat source, *Int. J. Heat Mass Transfer* **6**, 597 (1963).
7. K. Brodowicz and W. T. Kierkus, Experimental investigation of laminar free convection in air above a horizontal wire with constant heat flux, *Int. J. Heat Mass Transfer* **9**, 81 (1966).
8. R. J. Forstrom and E. M. Sparrow, Experiments on the buoyant plume above a heated horizontal wire, *Int. J. Heat Mass Transfer* **10**, 321 (1967).

9. A. W. Schorr and B. Gebhart, An experimental investigation of natural convection wakes above a line heat source, *Int. J. Heat Mass Transfer* **13**, 557 (1970).
10. Y. N. Lyakhov, Experimental investigation of free convection above a heated horizontal wire, *Zh. Prikl. Mekh. Tekh. Fiz.* **11**, 169. [Translated in *J. Applied Mech. Tech. Physics* **11**, 355 (1970).]
11. K. Miyabe and T. Katsuhara, Experimental investigation of the swaying plume above a heated horizontal cylinder, *Mem. Kyushu Inst. Technol.* **2**, 9 (1972).
12. L. Pera and B. Gebhart, On the stability of laminar plumes: some numerical solutions and experiments, *Int. J. Heat Mass Transfer* **14**, 975 (1971).
13. B. Gebhart, Instability, transition and turbulence in buoyancy induced flows, *Ann. Rev. Fluid Mech.* **5**, 213 (1973).
14. S. E. Haaland and E. M. Sparrow, Stability of buoyant boundary layers and plumes, taking into account of non parallelism of the basic flows, *J. Heat Transfer* **95**, 295 (1973).
15. R. P. Dring and B. Gebhart, A theoretical investigation of disturbance amplification in external natural convection, *J. Fluid Mech.* **34**, 551 (1969).
16. R. Mahajan and B. Gebhart, Calculations of plane plume stability characteristics. To be submitted.
17. H. Rouse, C. S. Yih and H. W. Humphreys, Gravitational convection from a boundary source, *Tellus* **4**, 21 (1952).
18. S. L. Lee and H. W. Emmons, A study of natural convection above a line fire, *J. Fluid Mech.* **11**, 353 (1961).
19. Y. Jaluria and B. Gebhart, On transition mechanism in vertical natural convection flow. To be submitted.
20. B. Gebhart and C. Knowles, Design and adjustment of a 20 cm Mach–Zehnder interferometer, *Rev. Scient. Instrum.* **37**, 12 (1966).
21. B. Gebhart and L. Pera, Mixed convection from long horizontal cylinders, *J. Fluid Mech.* **45**, 49 (1970).
22. G. G. Gubareff, J. E. Janseen and P. H. Torborg, *Thermal Radiation Properties Survey*, 2nd edn. Honeywell Regulator, Minneapolis (1960).